ADVANCED MATERIALS
www.advmat.de

Programmable Reversible Shape Transformation of Hydrogels Based on Transient Structural Anisotropy

Kangkang Liu, Yue Zhang, Heqing Cao, Haonan Liu, Yuhui Geng, Wenhua Yuan, Jian Zhou, Zi Liang Wu, Guorong Shan, Yongzhong Bao, Qian Zhao, Tao Xie, and Pengju Pan**

Stimuli-responsive shape-transforming hydrogels have shown great potential toward various engineering applications including soft robotics and microfluidics. Despite significant progress in designing hydrogels with ever more sophisticated shape-morphing behaviors, an ultimate goal yet to be fulfilled is programmable reversible shape transformation. It is reported here that transient structural anisotropy can be programmed into copolymer hydrogels of *N*-isopropylacrylamide and stearyl acrylate. Structural anisotropy arises from the deformed hydrophobic domains of the stearyl groups after thermomechanical programming, which serves as a template for the reversible globule-to-coil transition of the poly(*N*-isopropylacrylamide) chains. The structural anisotropy is transient and can be erased upon cooling. This allows repeated programming for reversible shape transformation, an unknown feature for the current hydrogels. The programmable reversible transformation is expected to greatly extend the technical scope for hydrogel-based devices.

Stimuli-responsive shape changing polymers have shown significant potential in diverse applications, such as soft actuators,[1–6] biomedical devices,[7,8] and flexible electronics.[9] Composed of a crosslinked water-swollen network, stimuli-responsive hydrogels exhibit excellent biocompatibility and unique transport property similar to biological tissues. General mechanism for shape transformation of the hydrogels relies on the variation of affinity between water molecules and polymer chains.[7] Responsive hydrogels with homogeneous structures can only exhibit simple shape changes, such as isotropic volume shrinkage/expansion. More complex shape morphing, such as bending, twisting, buckling, and even snapping[10–16] can be realized by introducing the spatial heterogeneity including chemical composition, crosslinking density, and filler orientation.[17–22] The above shape morphing behaviors are generally reversible but nonprogrammable, that is, the shape morphing pathways cannot be altered once the material fabrication process is completed.

Shape-memory hydrogels exhibit an opposite set of behavior.[23,24] They can be fixed into arbitrary temporary shapes and revert to the original shape on demand. This is defined as programmable shape shifting since the shifting pathway can be defined and altered via the programming procedure. The molecular mechanisms that allow locking and release of the shapes include melting transition,[25–27] reversible molecular interactions (or molecular switches),[28,29] and hydrophobic interactions.[30] For this type of behavior, a permanent shape does not revert back to the temporary shape unless an external force is imposed in a reprogramming step. Correspondingly, this is a programmable but not reversible shape shifting behavior. Hydrogels enabling programmable reversible shape transformation are still absent.

Solid polymers that can undergo programmable reversible shape shifting (i.e., two-way shape memory) have been recently revealed.[24,31] Most typically, such materials possess two separated (or a broad) crystalline melting transitions.[32–34] The high-melting-transition phase is utilized to introduce network anisotropy for programming, whereas heating and cooling across the low-melting-transition results in reversible shape transformation by way of crystallization-induced elongation and melting-induced contraction. As attractive as this shape shifting behavior is, the underlying mechanism is unfortunately not applicable for hydrogels which are composed of mostly water.

In this work, we have realized programmable reversible shape transformation of hydrogels, which was based on a previously unknown mechanism called transient structural anisotropy. These hydrogels are based on copolymers of *N*-isopropylacrylamide (NIPAM), stearyl acrylate (SA), and *N*,*N*′-methylenebisacrylamide (MBA) (**Figure 1**a). Herein, MBA serves as a crosslinker and is fixed at 2.5 mol% of total NIPAM

K. Liu, Y. Zhang, H. Cao, H. Liu, Y. Geng, W. Yuan, J. Zhou, Prof. G. Shan, Prof. Y. Bao, Prof. Q. Zhao, Prof. T. Xie, Prof. P. Pan
State Key Laboratory of Chemical Engineering
College of Chemical and Biological Engineering
Zhejiang University
Hangzhou 310027, P. R. China
E-mail: qianzhao@zju.edu.cn; panpengju@zju.edu.cn
Prof. Z. L. Wu
Key Laboratory of Macromolecular Synthesis and Functionalization of Ministry of Education
Department of Polymer Science and Engineering
Zhejiang University
Hangzhou 310027, P. R. China
Prof. Q. Zhao, Prof. T. Xie
ZJU-Hangzhou Global Scientific and Technological Innovation Center
Hangzhou 311215, P. R. China
The ORCID identification number(s) for the author(s) of this article can be found under https://doi.org/10.1002/adma.202001693.

DOI: 10.1002/adma.202001693

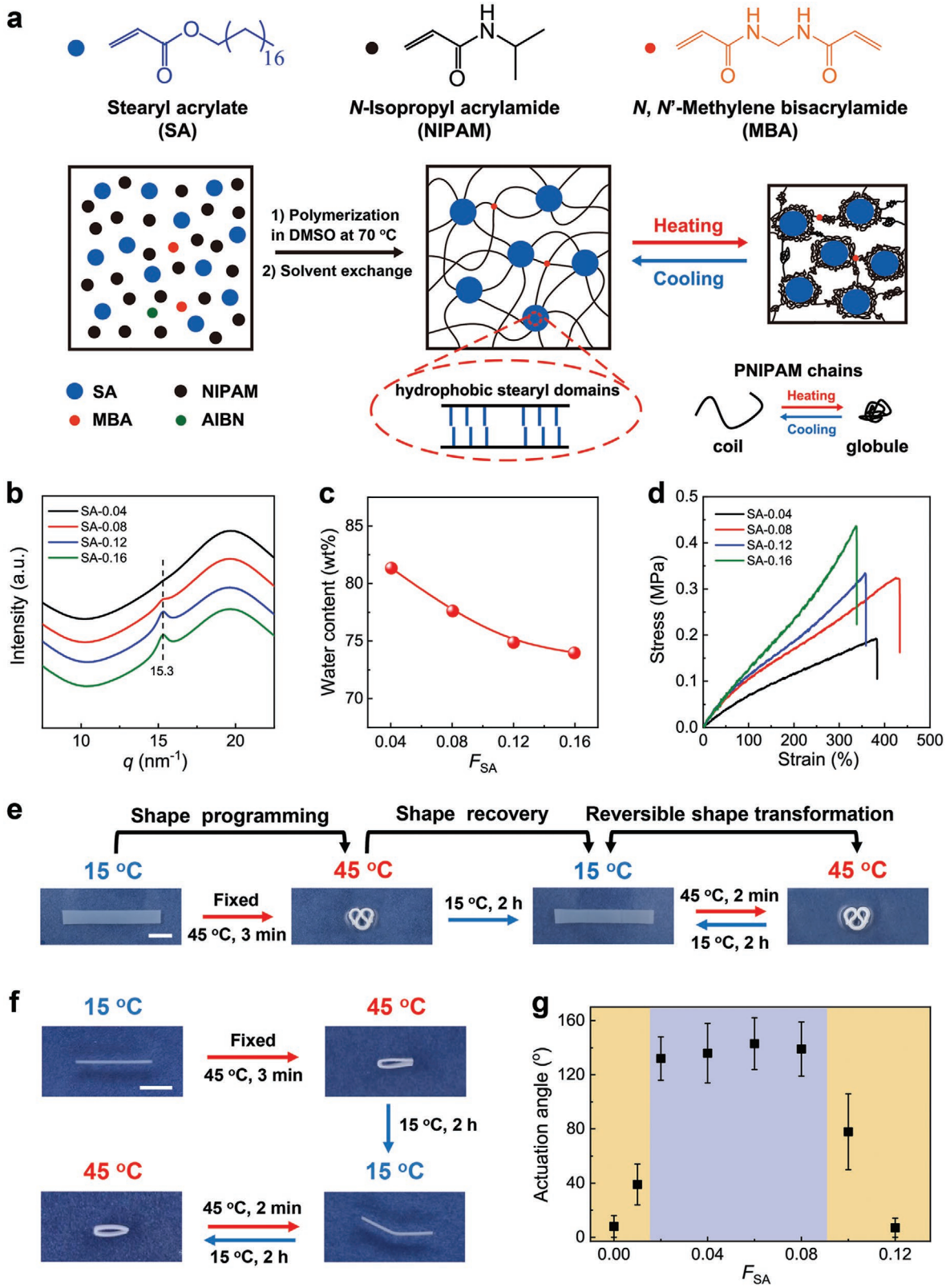

Figure 1. Synthesis, properties, and reversible shape transformation of P(NIPAM-*co*-SA) hydrogels. a) Schematics for the synthesis and thermosensitive transition of hydrogels. b) WAXS profiles, c) water content at 15 °C, and d) mechanical properties of the hydrogels with various F_{SA}. e) Images showing reversible shape transformation of the SA-0.08 hydrogel with a flat strip in 15 °C water and an "Ω" shape in 45 °C water. Scale bar: 1 cm. f) Reversible angle change of the SA-0.08 hydrogel in 15 and 45 °C water. Scale bar: 0.5 cm. g) Actuation angle of the hydrogels with various F_{SA}.

and SA monomers. For simplicity, the hydrogels are denoted as SA-F_{SA} with F_{SA} being the feed molar fraction of SA in the monomer mixture. Detailed synthetic procedures are presented in the Supporting Information. Two features are noteworthy in these hydrogels: 1) the melting transition of stearyl segments; 2) the thermoresponsiveness of the poly(*N*-isopropylacrylamide) (PNIPAM) chains which corresponds to the volume phase transition (VPT) of the hydrogels. We note that these two features are individually well known for imparting shape-memory functions into hydrogels. The melting transition is the basis for the cooling-induced shape fixing and heating-induced recovery.[25] The VPT, which coincides with its lower critical solution transition (LCST), forms an opposite shape-memory behavior, namely heating-induced shape fixing and cooling-induced recovery.[30,35] Of importance in the current context is that both these shape-memory behaviors are irreversible. Nevertheless, combination of these two common structural features/transitions in the same hydrogel is quite unusual. We illustrate hereafter that the synergetic interplay between these two transitions allows manipulating the molecular conformation of the hydrogels in an unusual manner to enable a highly versatile shape shifting behavior.

Microstructures of swollen hydrogels were first analyzed by wide- and small-angle X-ray scattering (WAXS, SAXS). In the WAXS profiles (Figure 1b), all the hydrogels show a broad scattering of water at $q = 19.7$ nm^{-1}. A characteristic peak appears at $q = 15.3$ nm^{-1} (lattice spacing, $d = 2\pi/q = 0.41$ nm) and intensifies with higher F_{SA}, suggesting that it originates from the hydrophobic domains of stearyl groups.[36] SAXS profiles of all the hydrogels display a notable scattering peak at $q = 1.2$–1.3 nm^{-1} (Figure S1, Supporting Information), indicating the formation of stearyl layers with the thickness of 5.0–5.2 nm ($2\pi/q$) in the hydrophobic domains.[36] The shift of the scattering peak verifies that the stearyl layers become more compact with the increase of F_{SA}. Physical properties of the hydrogels are influenced by F_{SA}. The SA-0.02 hydrogel was transparent, yet hydrogels with higher F_{SA} became opaque (Figure S2, Supporting Information). As F_{SA} increases from 0.04 to 0.16, the water content at 15 °C decreases from 81% to 74% (Figure 1c). The increase in F_{SA} also led to the enhancement of mechanical strength (Figure 1d), presumably due to the denser physical crosslinking.

The VPT temperature of SA-0.08 hydrogels is around 30 °C (Figure S3, Supporting Information), slightly lower than that of the common PNIPAM hydrogels (≈34 °C) due to the presence of hydrophobic stearyl moieties.[7] PNIPAM chains are hydrophilic and adopt the random coil conformation at a low temperature, due to the hydration of isopropyl groups. This hydration state is destroyed as the temperature exceeds VPT temperature, resulting in the coil-to-globule transition of chain conformation (Figure 1a).[37]

We proceed to explore the shape morphing behaviors of the hydrogels. A rectangular sample of SA-0.08 hydrogel was deformed at 15 °C and fixed into a temporary "Ω" shape at 45 °C (Figure 1e). This temporary shape recovered into the original rectangular shape after being reimmersed in 15 °C water for 2 h. This above shape-memory behavior is fully expected with the LCST serving as the switching mechanism. What is surprising and totally unexpected is the following. When the recovered rectangular shape was immersed to the 45 °C water again, it returned to the "Ω" shape in 2 min (Movie S1, Supporting Information). Repeated switching between 45 and 15 °C allows reversible shape transformation between these two shapes for at least ten cycles (Figure S4, Supporting Information), showing a robust programmable and reversible shape shifting behavior.

Two experimental phenomena are worth noting here. First, the stearyl domains were at a crystalline state under the programming temperature (45 °C), as proved by WAXS data (Figure S5a, Supporting Information). Intriguingly, the reversible actuation worked well as long as the programming temperature is higher than the VPT temperature of hydrogel, regardless of the crystalline or melting state of stearyl domains. Good reversible actuation was also achieved when the programing temperature (e.g., 70 °C) was much higher than the melting temperature of stearyl domains (Figure S6, Supporting Information), because the stearyl domains still existed in the melt state (Figure S5b, Supporting Information). Second, the reversible actuation was also workable upon heating and cooling the hydrogel in silicone oil, under which conditions the absorption or release of water did not happen (Figure S7, Supporting Information). This is a strong evidence that the conformational change of PNIPAM chains, rather than the volume change of hydrogel, was the primary mechanism behind the reversible actuation.

To understand the role of stearyl domains in the shape transformation, the shape changing capability of hydrogels with various F_{SA} was quantitatively characterized using a bending deformation mode. Hydrogel strips were programmed via folding in the middle. All the hydrogels with various F_{SA}'s showed good one-way shape-memory capability with the high fixity ratios ($R_f > 84\%$) and recovery ratios ($R_r > 85\%$) (Figure S8, Supporting Information). However, only the hydrogels with medium F_{SA} (0.02–0.08) displayed the good reversible actuation performance. Figure 1f shows that the programmed hydrogel strip (SA-0.08) possesses a reversible angle change of ≈140°, the extent of this reversible actuation is significantly superior to existing two-way shape-memory polymers.[32–34] Good reversible actuation was not observed for the hydrogels without stearyl groups (SA-0) or with too much stearyl groups (e.g., SA-0.12) (Figure 1g). Unless otherwise noted, we hereafter focus on the SA-0.08 hydrogel to further probe the reversible actuation performance.

Figure 2a shows the reversible actuation kinetics of the SA-0.08 hydrogel, corresponding to the experiment in Figure 1f. The bending angle changed from 160° to nearly zero in 45 °C water for 2 min and then gradually recovered to 160° in 15 °C water for 30–60 min. The actuation is reversible upon multicycling with some cycle to cycle upshifting in the bending angle at 45 °C (Figure 2b). The water content altered only slightly between 78% at 15 °C and 72% at 45 °C during the repeated cycles (Figure 2c). We emphasize that the shape morphing of hydrogel was much faster than the deswelling equilibrium at 45 °C. The shape morphing took only 2 min but the equilibrium of deswelling needed ≈2 h at 45 °C (Figure S9, Supporting Information). This is consistent with our experiments conducted in silicone oil, with both suggesting that the reversible actuation is independent of the swelling/deswelling process.

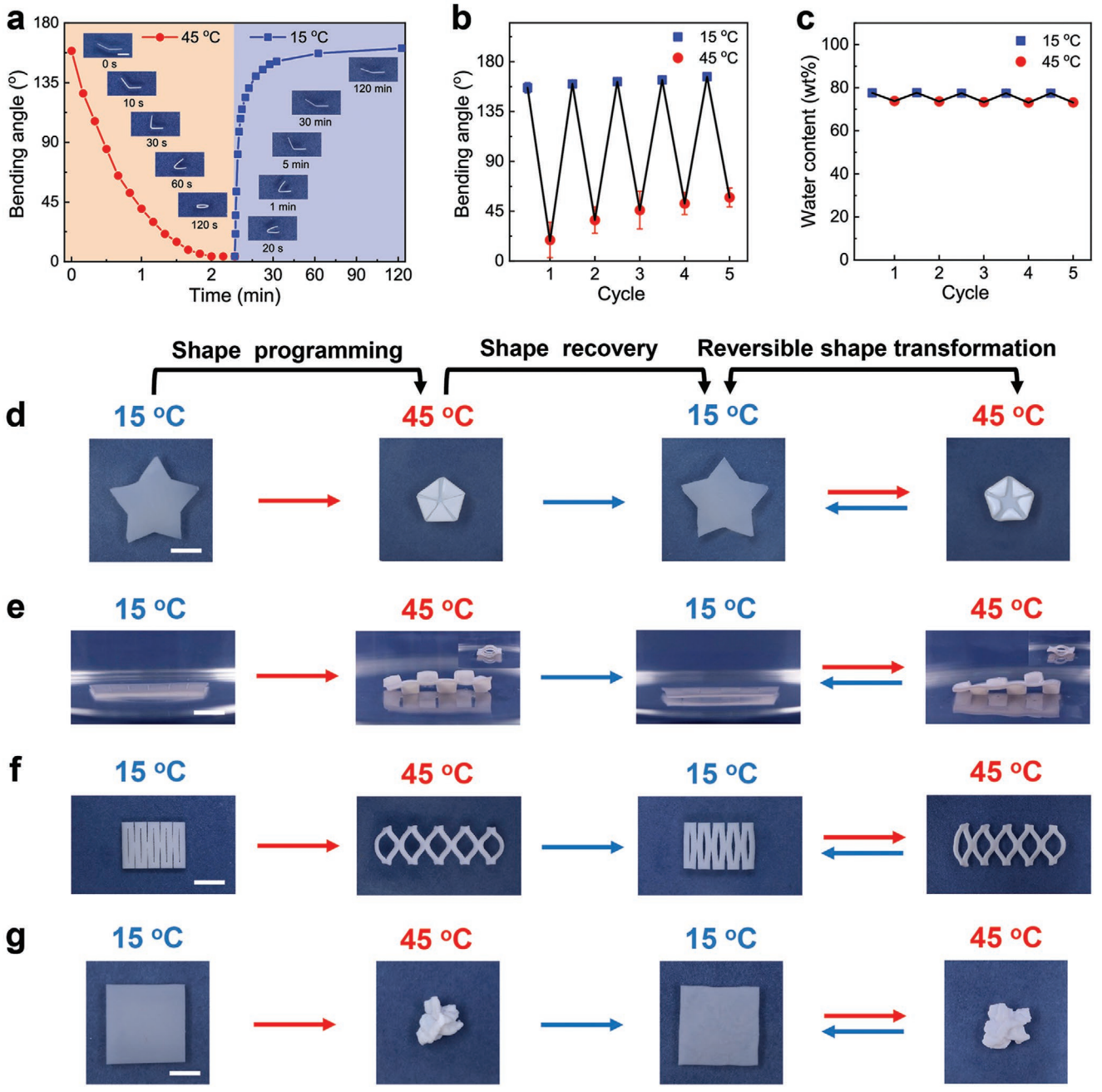

Figure 2. Reversible shape transformation of the SA-0.08 hydrogel in 15 and 45 °C water. a) Actuation kinetics in one bending cycle. Insets are the images taken during the actuation process. b,c) Bending angle and water content during repeated cycles when the hydrogel was switched between 15 °C water for 2 h and 45 °C water for 2 min. d–g) Images showing diversified shape transformation of hydrogel sheets (origami star, kirigami array, and randomly kneaded sheet). Scale bar: 1 cm.

The programmability allows the hydrogels to reversibly shift between various shapes (Figure 2d–g; and Movies S2–S4, Supporting Information). The origami star in Figure 2d can be regarded as locally programming since only the folded areas are programmed. Notably, this easy access to diverse and complex transformation via mechanical programming is not offered by any previous hydrogel systems. Intriguingly, the reversible actuation can be completely erased when a programmed hydrogel was immersed in 15 °C water for a long time (e.g., 30 h) (Figure S10, Supporting Information). This establishes the basis for reprogramming. As shown in **Figure 3**a, the reversible shape changing of hydrogel between an "Ω" shape and a flat strip could be erased and then reprogrammed into the transformation between helix and flat shapes. The hydrogels could be reprogrammed for more than 10 times without damage and the reversible shape transformation still worked well after 10 times of erasing processes. The same principle can be applied to reversibly manipulate the surface microstructures.

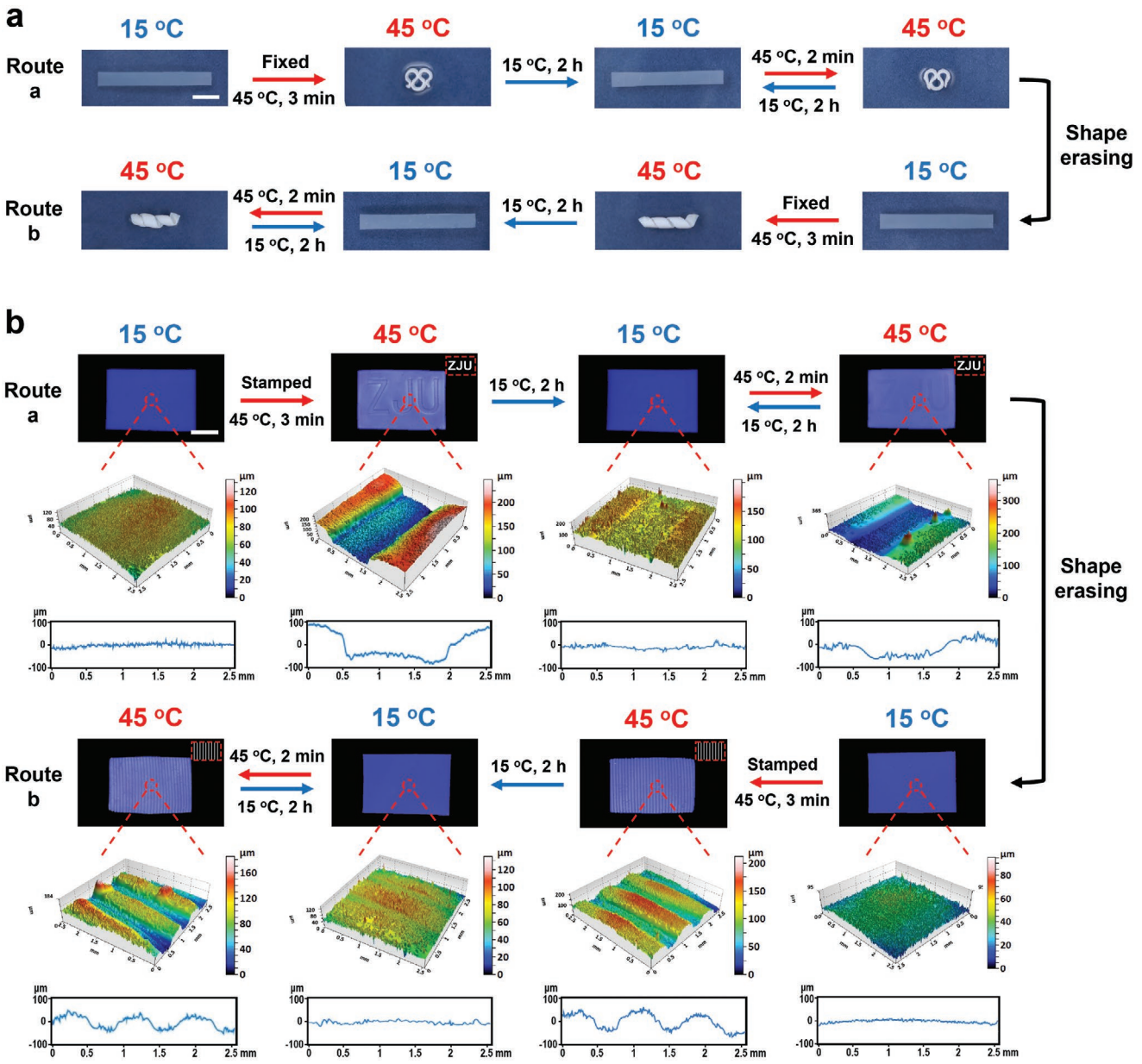

Figure 3. Reprogramming of reversible shape transformation of the SA-0.08 hydrogel. a) Reprogrammability of macroscopic shapes from an "Ω" shape to a helix shape. b) Reprogrammability of surface patterns from "ZJU" characters (route a) to a grating pattern (route b). The hydrogel was dyed by crystal violet for better visualization. Scale bar: 1 cm.

A pattern of "ZJU" characters was embossed and temporarily fixed at 45 °C (route a of Figure 3b). The pattern became invisible after recovery for 2 h in 15 °C water. The "ZJU" pattern emerged again upon heating without external force, showing a reversible actuation nature. This reversible pattern transformation could be completely erased via long-time relaxation in cool water (Figure S11, Supporting Information). Afterward, new patterns (e.g., gratings) could be encoded and transformed reversibly in the thermal cycles (route b of Figure 3b).

To understand the underlying mechanism, we investigate how the recovery time in 15 °C cold water affects the shape transformation behavior of hydrogels. Long-time equilibration (≥12 h) led to fully angle recovery (Figure S12, Supporting Information) but eliminated the reversible actuation ability of hydrogel at high temperature (**Figure 4**a). X-ray scattering characterizations also verified the slow structural relaxation and transition in cold water. Figure 4b shows that the scattering of water ($q = 19.7\ nm^{-1}$) intensified gradually after the temperature changed from 45 to 15 °C and the microstructure of hydrogel recovered to the initial state after holding in cold water for nearly 30 h. As shown in Figure 4c, the original hydrogel varied from the isotropic to orientated structure after being stretched and fixed into a programmed shape at 45 °C. Structural orientation weakened but persisted after recovering at 15 °C for

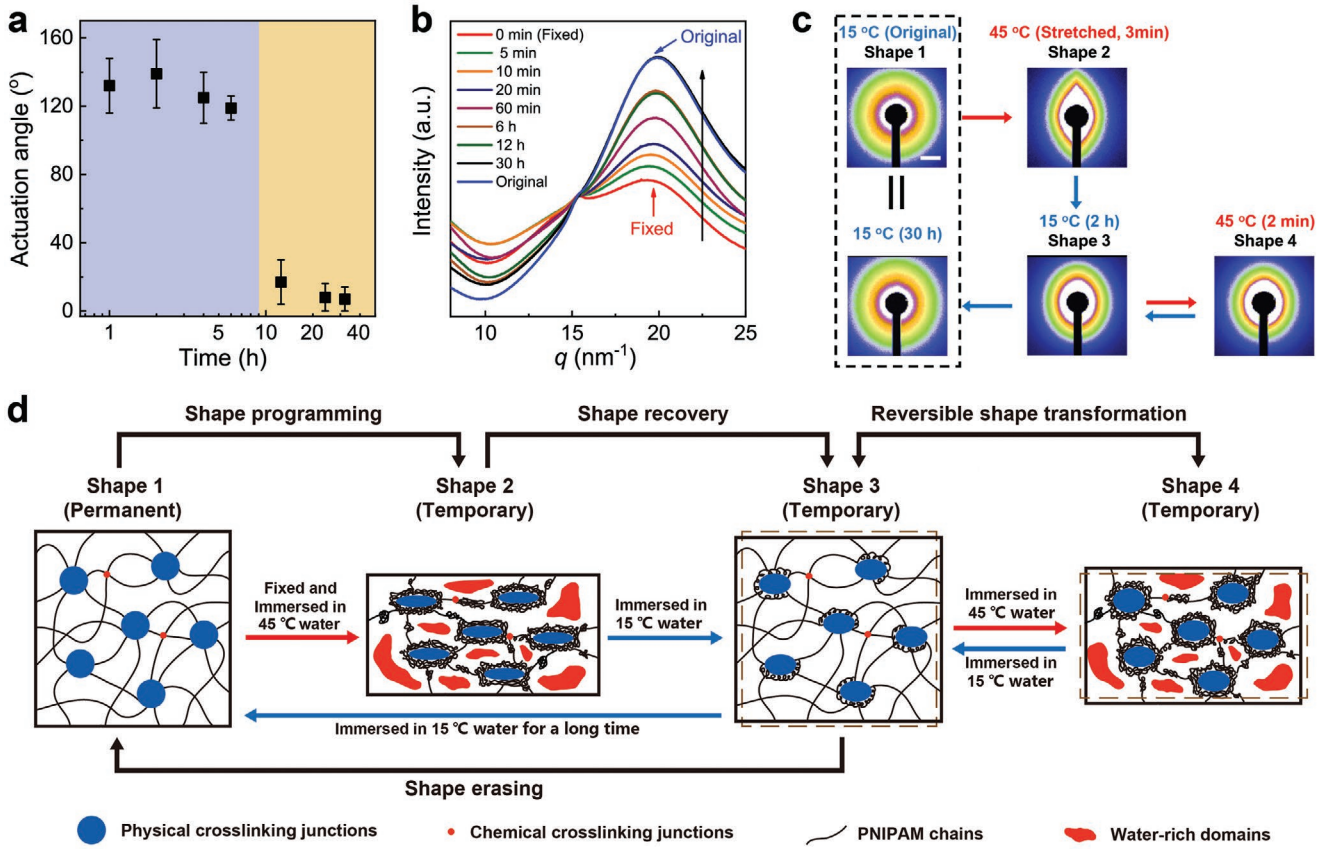

Figure 4. Mechanistic study of the reversible shape transformation. a) Actuation angles of the SA-0.08 hydrogel at 45 °C (2 min) after immersed in 15 °C water for different times. b) WAXS profiles of the SA-0.08 hydrogel immersed in 15 °C water for different times after fixed in 45 °C water for 3 min. c) 2D SAXS images showing the microstructural evolution of the SA-0.08 hydrogel during the shape transformation process. The hydrogel was programmed by stretching to 200% strain in 45 °C water for 3 min. Scale bar of q: 0.1 nm^{-1}. d) Schematic representation showing a proposed mechanism for the reversible shape transformation.

2 h, which completely disappeared after the long-time recovery (e.g., 30 h). Accordingly, we can conclude that the hydrogel did not recovery to the original (or equilibrated) state but in the transient state after immersing in cold water for 2 h. This conclusion is consistent with our finding that the shapes of hydrogels are different after recovering in cold water for different times (e.g., 2 and 30 h) (Figure 1f).

Based on the abovementioned results, we propose a mechanism (Figure 4d) for the reversible actuation of hydrogel. For the starting hydrogel (shape 1, original shape) in cold water, PNIPAM chains are in the relaxed random coil state and the network is isotropic. During programming in hot water, the hydrophobic stearyl domains became stretched and the collapsed PNIPAM in their globular state would aggregate around the stearyl domains due to the hydrophobic interactions. This enables the temporary fixation of the deformed stearyl domains and the macroscopic shape (shape 2, programmed shape). At this state, PNIPAM globules also exhibit anisotropy due to the chain stretching and water molecules are excluded by the PNIPAM hydrophobic globules to form surrounding water-rich domains. Upon cooling, the PNIPAM globules absorb more water and relax slowly to the hydrophilic coils, together with the disorientation of PNIPAM chains. The transition cannot be completed within a short recovery time (e.g., 2 h), which is most likely because the presence of the hydrophobic stearyl domains decelerates this conformational transition. Consequently, a transient state exists in which the orientation of residual PNIPAM globules and stearyl domains are kinetically trapped, corresponding to shape 3. When the kinetically-trapped transient hydrogel is immersed in hot water again, the coil-to-globule transition of PNIPAM chains tends to occur along the orientated direction of the residual PNIPAM globules. Accordingly, the hydrogel changes anisotropically toward the programmed shape (shape 4), displaying an overall programmable reversible actuation. However, if the material is exposed to cold water for a sufficiently long time (e.g., 30 h), it reaches the equilibrium state with the isotropic and fully relax chain structure. This would erase the previously encoded reversible actuation and enable reprogrammability. Notably, the role of crystalline or melted hydrophobic stearyl domains is to guide the orientation of the surrounding PNIPAM chains in the cooling-induced globule-to-coil transition. In other words, the reversible actuation is mainly caused by the thermoresponsive conformation change of PNIPAM chains, with the stearyl domains providing a transient template for programming.

In conclusion, we devised the materials/processes that allow realization of programmable reversible shape transformation in thermoresponsive hydrogels with hydrophobically associated

domains. The programmable nature results in easy access to diversified transformation of macroscopic shapes, extending the scope beyond current hydrogel systems. This versatile shape shifting behavior hinges heavily on the chemical composition of the hydrogels, with the content of the hydrophobic stearyl groups playing a critical role. Insufficient or excessive amount of stearyl groups depresses or even eliminates the reversible actuation. The reversible actuation of hydrogel can be erased via long-time relaxation in cold water, which establishes the basis for reprogrammability. Mechanistically, the reversible shape transformation relies on the oriented globule-to-coil transition of PNIPAM chains along the deformed hydrophobic domains induced via programming. The programmable reversible actuation of hydrogels expands significantly the scope for designing future smart hydrogel-based devices.

Supporting Information

Supporting Information is available from the Wiley Online Library or from the author.

Acknowledgements

K.L. and Y.Z. contributed equally to this work. The authors thank the following programs for the financial support: the National Natural Science Foundation of China (Nos. 51822307 and 21674095), the Natural Science Foundation of Zhejiang Province (Nos. LR16E030003 and LR18E030001), Fundamental Research Funds for the Central Universities (No. 2018RC020), and the State Key Laboratory of Chemical Engineering (No. SKLChE-16Z). The authors also thank the BL16B1 beamline of SSRF for WAXS and SAXS measurements.

Conflict of Interest

The authors declare no conflict of interest.

Keywords

coil–globule transitions, programmable shape transformation, reversible shape transformation, shape memory, transient anisotropy, thermosensitive hydrogels

Received: March 10, 2020
Revised: April 23, 2020
Published online: May 28, 2020

[1] L. Ionov, *Mater. Today* **2014**, *17*, 494.
[2] X. Liu, J. Liu, S. Lin, X. Zhao, *Mater. Today* **2020**, https://doi.org/10.1016/j.mattod.2019.12.026.
[3] T. Matsuda, R. Kawakami, R. Namba, T. Nakajima, J. P. Gong, *Science* **2019**, *363*, 504.
[4] A. Sidorenko, T. Krupenkin, A. Taylor, P. Fratzl, J. Aizenberg, *Science* **2007**, *315*, 487.
[5] H. Yuk, S. Lin, C. Ma, M. Takaffoli, N. X. Fang, X. Zhao, *Nat. Commun.* **2017**, *8*, 14230.
[6] J.-Y. Sun, X. Zhao, W. R. K. Illeperuma, O. Chaudhuri, K. H. Oh, D. J. Mooney, J. J. Vlassak, Z. Suo, *Nature* **2012**, *489*, 133.
[7] Y. Qiu, K. Park, *Adv. Drug Delivery Rev.* **2001**, *53*, 321.
[8] Y. S. Zhang, A. Khademhosseini, *Science* **2017**, *356*, eaaf3627.
[9] C. Keplinger, J.-Y. Sun, C. C. Foo, P. Rothemund, G. M. Whitesides, Z. Suo, *Science* **2013**, *341*, 984.
[10] J.-H. Na, A. A. Evans, J. Bae, M. C. Chiappelli, C. D. Santangelo, R. J. Lang, T. C. Hull, R. C. Hayward, *Adv. Mater.* **2015**, *27*, 79.
[11] C. Ma, T. Li, Q. Zhao, X. Yang, J. Wu, Y. Luo, T. Xie, *Adv. Mater.* **2014**, *26*, 5665.
[12] Z. L. Wu, M. Moshe, J. Greener, H. Therien-Aubin, Z. Nie, E. Sharon, E. Kumacheva, *Nat. Commun.* **2013**, *4*, 1586.
[13] Y. Zhang, J. Liao, T. Wang, W. Sun, Z. Tong, *Adv. Funct. Mater.* **2018**, *28*, 1707245.
[14] G. Wu, Y. Xia, S. Yang, *Soft Matter* **2014**, *10*, 1392.
[15] C. Yu, Z. Duan, P. Yuan, Y. Li, Y. Su, X. Zhang, Y. Pan, L. L. Dai, R. G. Nuzzo, Y. Huang, H. Jiang, J. A. Rogers, *Adv. Mater.* **2013**, *25*, 1541.
[16] Q. Zhao, X. Yang, C. Ma, D. Chen, H. Bai, T. Li, W. Yang, T. Xie, *Mater. Horiz.* **2016**, *3*, 422.
[17] M. L. Smith, C. Slone, K. Heitfeld, R. A. Vaia, *Adv. Funct. Mater.* **2013**, *23*, 2835.
[18] Z. J. Wang, C. N. Zhu, W. Hong, Z. L. Wu, Q. Zheng, *Sci. Adv.* **2017**, *3*, e1700348.
[19] J. Kim, J. A. Hanna, M. Byun, C. D. Santangelo, R. C. Hayward, *Science* **2012**, *335*, 1201.
[20] Y. S. Kim, M. Liu, Y. Ishida, Y. Ebina, M. Osada, T. Sasaki, T. Hikima, M. Takata, T. Aida, *Nat. Mater.* **2015**, *14*, 1002.
[21] A. S. Gladman, E. A. Matsumoto, R. G. Nuzzo, L. Mahadevan, J. A. Lewis, *Nat. Mater.* **2016**, *15*, 413.
[22] C. Yao, Z. Liu, C. Yang, W. Wang, X.-J. Ju, R. Xie, L.-Y. Chu, *Adv. Funct. Mater.* **2015**, *25*, 2980.
[23] F. Liu, M. W. Urban, *Prog. Polym. Sci.* **2010**, *35*, 3.
[24] Q. Zhao, H. J. Qi, T. Xie, *Prog. Polym. Sci.* **2015**, *49–50*, 79.
[25] Y. Osada, A. Matsuda, *Nature* **1995**, *376*, 219.
[26] Z. Zhao, K. Zhang, Y. Liu, J. Zhou, M. Liu, *Adv. Mater.* **2017**, *29*, 1701695.
[27] Z. Zhao, S. Zhuo, R. Fang, L. Zhang, X. Zhou, Y. Xu, J. Zhang, Z. Dong, L. Jiang, M. Liu, *Adv. Mater.* **2018**, *30*, 1804435.
[28] W. Lu, X. Le, J. Zhang, Y. Huang, T. Chen, *Chem. Soc. Rev.* **2017**, *46*, 1284.
[29] Y. Han, T. Bai, Y. Liu, X. Zhai, W. Liu, *Macromol. Rapid Commun.* **2012**, *33*, 225.
[30] X. Hu, D. Zhang, S. S. Sheiko, *Adv. Mater.* **2018**, *30*, 1707461.
[31] T. H. Ware, M. E. McConney, J. J. Wie, V. P. Tondiglia, T. J. White, *Science* **2015**, *347*, 982.
[32] M. Behl, K. Kratz, J. Zotzmann, U. Nöchel, A. Lendlein, *Adv. Mater.* **2013**, *25*, 4466.
[33] J. Zhou, S. A. Turner, S. M. Brosnan, Q. X. Li, J.-M. Y. Carrillo, D. Nykypanchuk, O. Gang, V. S. Ashby, A. V. Dobrynin, S. S. Sheiko, *Macromolecules* **2014**, *47*, 1768.
[34] B. Jin, H. Song, R. Jiang, J. Song, Q. Zhao, T. Xie, *Sci. Adv.* **2018**, *4*, eaao3865.
[35] C. C. Wang, W. M. Huang, Z. Ding, Y. Zhao, H. Purnawali, *Compos. Sci. Technol.* **2012**, *72*, 1178.
[36] Y. Geng, X. Y. Lin, P. Pan, G. Shan, Y. Bao, Y. Song, Z. L. Wu, Q. Zheng, *Polymer* **2016**, *100*, 60.
[37] X. Wang, X. Qiu, C. Wu, *Macromolecules* **1998**, *31*, 2972.